

PARAMETRIC DESIGN AND MULTI-OBJECTIVE OPTIMIZATION OF EXHAUST NOZZLE FOR GAS TURBINE ENGINES

Thai Q. Dinh, Hung X. Vu, Anh C. Pham & Lanh D. Chu

Viettel Aerospace Institute (VTX), Hanoi, Vietnam

Email: thaiquangdink@gmail.com, thaidq5@viettel.com.vn.

Abstract

The design and optimization of nozzles in gas turbine engines play a critical role in enhancing overall engine efficiency, thrust output, and operational reliability. In modern aerospace propulsion systems, convergent nozzles are essential components that accelerate exhaust gases to generate thrust, particularly in applications where subsonic flow is predominant. However, achieving optimal performance requires balancing multiple geometric parameters to maximize key aerodynamic metrics while adhering to manufacturing and engine integration constraints. This study addresses the challenge of designing and optimizing a convergent exhaust nozzle for gas turbine engines, integrating computational fluid dynamics (CFD) simulations with advanced sensitivity analysis and optimization techniques. The primary purpose of this work is to develop a systematic methodology for refining nozzle geometry to achieve superior flow characteristics, thereby improving engine performance metrics like discharge coefficient (Cd), gross thrust coefficient (Cfg), and exit total pressure. By leveraging parametric modeling and automated optimization workflows, this research aims to provide engineers with actionable insights into nozzle design trade-offs, ultimately contributing to more efficient and sustainable gas turbine systems.

The technical foundation of this investigation is in a parametric approach to nozzle geometry definition and evaluation. The convergent nozzle in this work is characterized by five geometric input parameters: nozzle length, inner cone angle, inner cone radius (representing the radius at the tip of the inner cone), and two outer case radius. These parameters were selected based on their direct influence on flow convergence, boundary layer development, and pressure recovery within the nozzle. A pre-determined exit diameter was imposed as a fixed constraint to simulate real-world design scenarios, such as those encountered in engine retrofits or modular turbine assemblies. The simulation framework employed ANSYS Fluent, a robust CFD solver, to model the compressible flow through the nozzle under representative operating conditions, including inlet total pressure, temperature, and mass flow rates typical of gas turbine exhaust streams. The CFD model incorporated the k-ϵ turbulence model for accurate prediction of compressible flow inside the nozzle and the incompressible flow outside the domain, with quadrilateral mesh ensuring solution accuracy within 1% convergence criteria. Output parameters extracted from the simulations included the coefficient of discharge (Cd), defined as the ratio of actual mass flow rate obtained from CFD to the ideal isentropic mass flow rate; the gross thrust coefficient (Cfg), calculated as the ratio of computed thrust to the ideal thrust under isentropic expansion; and the exit total pressure, which quantifies pressure losses and recovery efficiency.

To extend beyond single-point CFD evaluations, a surrogate-assisted multi-objective optimization workflow was developed. An initial sensitivity analysis was conducted to identify the most influential geometric parameters on the nozzle performance metrics. Advanced Latin Hypercube Sampling was used to generate representative design points across the feasible design space. Response surface models, including polynomial regression and Kriging-based metamodels, were then constructed to approximate the relationships between the geometric input parameters and aerodynamic output responses. The optimization process employed the Metamodel of Optimal Prognosis (MOP) to search for improved nozzle configurations while reducing the number of required CFD simulations. The optimization objectives were defined to maximize the discharge coefficient, gross thrust coefficient, thrust, and exit total pressure recovery, while maintaining geometric feasibility and avoiding unfavorable flow behavior such as excessive adverse pressure gradients.

Preliminary results from the CFD and optimization campaigns demonstrate promising enhancements in nozzle performance. Baseline designs, derived from empirical correlations, yielded Cd values around 0.97 and Cfg around 0.96, with exit total pressures exhibiting losses of approximately 1.5-1.6% relative to inlet conditions. Through sensitivity analysis, the inner cone angle and nozzle length emerged as dominant factors, contributing over 60% to variance in Cd and Cfg, while the inner cone radius had a pronounced effect on exit pressure recovery. The optimized geometries, after 150-200 design iterations, achieved Cd improvements up to 0.98, Cfg up to 0.97, and exit total pressure increases, exhibiting losses of approximately 1.2-1.4% relative to inlet conditions. These gains were validated through detailed flow field visualizations and smoother velocity profiles in the optimized configurations.

Expected outcomes of this research include a validated optimization framework that can be extended to more complex nozzle configurations, such as convergent-divergent or variable-geometry nozzles in high-bypass turbofans. The methodology is anticipated to yield design guidelines for achieving Cd and Cfg values approaching unity, thereby enabling gas turbine engines with higher thrust and lower pressure losses.

Keywords: nozzle, gas turbine, parametric design, multi-objective optimization, sensitivity analysis, discharge coefficient, gross thrust coefficient.

1. Introduction

The exhaust nozzle is a critical component of a gas turbine engine because it converts the remaining thermal and pressure energy of the turbine-exit gas into a high-velocity jet. This acceleration process directly affects the generated thrust, engine back pressure, mass flow capacity, and overall propulsive performance. In a simple gas turbine engine, the nozzle is placed downstream of the turbine and acts as the final aerodynamic component before the exhaust gas is discharged to the ambient environment. Although the nozzle is geometrically simpler than compressors, turbines, or combustors, its aerodynamic performance strongly influences the matching between the engine core flow and the external environment. Therefore, nozzle design must satisfy not only thrust requirements but also flow-capacity, pressure-loss, reliability, manufacturing, and engine-integration constraints.

For many gas turbine applications operating in subsonic or moderately high-speed regimes, a convergent nozzle is commonly used because of its compact structure, simple manufacturing requirements, and ability to accelerate the exhaust flow efficiently. In a convergent nozzle, the flow area decreases from the inlet to the exit, causing the gas velocity to increase and the static pressure to decrease. When the nozzle pressure ratio reaches a critical value, the flow becomes choked, and the Mach number at the minimum area reaches unity. Under this condition, the mass flow rate is mainly governed by the nozzle throat or exit area, inlet total pressure, inlet total temperature, gas properties, and total pressure losses inside the nozzle [1]. Since the exit plane is also the minimum flow area in a convergent nozzle, the exit diameter becomes an important design constraint, particularly in practical engine retrofit, modular turbine assembly, or installation-limited applications.

The thrust produced by a nozzle depends on the mass flow rate, exit velocity, flight or reference velocity, and the pressure difference between the nozzle exit and the ambient environment [2]. In practical operation, the actual nozzle performance is lower than the ideal isentropic prediction because of viscous effects, boundary-layer development, local flow non-uniformity, wall curvature effects, and total pressure losses. These effects are commonly evaluated using aerodynamic performance coefficients such as the discharge coefficient and the gross thrust coefficient. The discharge coefficient (C_D) represents the ratio between the actual mass flow rate and the ideal isentropic mass flow rate, while the gross thrust coefficient, (C_{fg}), compares the actual gross thrust with the ideal thrust under the same reference conditions [3]. In addition, exit total pressure or total pressure loss is an important indicator of internal aerodynamic loss and pressure-recovery efficiency. A well-designed convergent nozzle should therefore provide high C_D, high C_{fg}, high thrust, and low total pressure loss simultaneously.

The design of a convergent exhaust nozzle is a multi-parameter aerodynamic problem. Important geometric variables may include nozzle length, convergence angle, inner cone radius, outer casing radii, inlet diameter, exit diameter, and wall-contour curvature. These parameters influence the internal acceleration process, boundary-layer growth, velocity distribution, pressure recovery, and loss

generation. Traditional preliminary design methods are often based on one-dimensional compressible-flow theory and empirical correction factors. Such methods are useful for estimating the required flow area, choked mass flow rate, ideal exit velocity, and ideal thrust. However, they cannot fully capture multidimensional flow phenomena and detailed geometric effects. For this reason, computational fluid dynamics has become an important tool for nozzle analysis and design, especially when the nozzle contour is described parametrically and multiple performance indicators must be evaluated simultaneously.

Reynolds-averaged Navier–Stokes CFD simulations are widely used in exhaust nozzle design because they provide detailed information about the internal flow field, including pressure distribution, Mach number, velocity profile, wall shear stress, separation tendency, and total pressure loss. CFD also enables direct extraction of engineering performance quantities such as mass flow rate, thrust, discharge coefficient, gross thrust coefficient, and exit total pressure. Compared with purely analytical methods, CFD-based design gives a more realistic representation of practical nozzle behavior, particularly when the flow is compressible, viscous, and affected by wall-contour variations. Therefore, CFD provides a suitable foundation for parametric design and optimization of convergent exhaust nozzles.

Previous studies have shown that parametric geometry definition is effective for aircraft-engine exhaust and nozzle design. Goulos et al. developed an integrated computational framework for the aerodynamic design and optimization of separate-jet exhaust systems for civil aero-engines. Their methodology combined engine performance analysis, parametric geometry definition, automated meshing, viscous compressible CFD simulation, design-space exploration, surrogate modeling, and optimization [4]. Although their study focused on separate-jet turbofan exhaust systems rather than a simple convergent nozzle, the methodology is highly relevant because it demonstrates how exhaust geometry can be represented by a limited number of design variables and systematically evaluated using CFD. Other studies have also emphasized CAD-based aerodynamic shape optimization, where nozzle geometry is parameterized in a way that preserves smoothness, manufacturability, and compatibility with surrounding engine structures [5].

In addition to geometry parameterization, optimization methods have become increasingly important in nozzle design. A common approach is design-space exploration using sampling techniques such as full-factorial design, Latin hypercube sampling, or advanced Latin hypercube sampling. These methods generate a set of representative design points over the feasible parameter space, allowing the influence of each design variable on the output responses to be assessed. Sensitivity analysis can then be used to identify the most influential parameters and reduce unnecessary design complexity. This step is particularly useful in nozzle optimization because geometric variables do not contribute equally to the final aerodynamic performance. For example, changes in nozzle length or cone angle may strongly affect discharge and thrust coefficients, while local radius parameters may have a stronger influence on pressure recovery and wall-flow behavior.

However, direct CFD-based optimization can be computationally expensive because each design evaluation requires geometry generation, meshing, solver execution, and post-processing. To reduce this cost, surrogate-based optimization has been widely adopted in aerodynamic design. In this approach, CFD results from a limited number of sampled designs are used to construct approximation models, such as polynomial response surfaces, Kriging models, radial basis functions, or neural-network-based metamodels. These surrogate models approximate the relationship between design variables and objective functions, allowing the optimizer to explore the design landscape more efficiently than with brute-force CFD simulation. Kriging-based and response-surface-based methods are especially useful for nozzle design because they can capture nonlinear relationships between geometric parameters and aerodynamic outputs while reducing the number of high-fidelity CFD evaluations required [6].

For multi-objective aerodynamic problems, evolutionary algorithms, Pareto-based optimization, Bayesian optimization, and adaptive metamodel methods have been applied to identify balanced design solutions. Adjoint-based optimization has also been applied to nozzle shape design, particularly for problems involving a large number of shape variables. Yerlikaya applied adjoint-based optimization

to a supersonic converging-diverging nozzle to improve thrust-related performance while satisfying geometric constraints [7]. Unlike single-objective optimization, multi-objective optimization does not produce only one optimum geometry. Instead, it provides a set of Pareto-optimal solutions that represent trade-offs among competing objectives. This is important for exhaust nozzle design because maximizing discharge coefficient, maximizing gross thrust coefficient, maximizing thrust, and minimizing total pressure loss may not always lead to the same geometry. For example, an aggressive contraction may increase acceleration and thrust but may also increase local pressure gradients and loss generation. Conversely, a smoother and longer nozzle may reduce total pressure loss but may not satisfy compactness or integration requirements. Therefore, a multi-objective approach is more suitable for identifying practical nozzle geometries that provide balanced aerodynamic performance.

Recent optimization frameworks integrated within commercial engineering environments also allow CFD, sensitivity analysis, surrogate modeling, and optimization to be combined in a single automated workflow. In the ANSYS ecosystem, OptiSLang provides tools for design of experiments, sensitivity analysis, response-surface construction, metamodel generation, and robust design evaluation. Techniques such as Advanced Latin Hypercube Sampling, polynomial regression, Kriging metamodels, and Adaptive Metamodel of Optimal Prognosis can be used to explore the design space and search for Pareto-optimal configurations with fewer CFD evaluations. This type of workflow is particularly suitable for preliminary and detailed nozzle design because it allows engineers to quantify the relationship between geometric variables and aerodynamic performance while considering design constraints and possible manufacturing variations.

Based on this background, the present study focuses on the parametric design and multi-objective optimization of a convergent exhaust nozzle for gas turbine engine applications. The nozzle geometry is defined using five input parameters: nozzle length, inner cone angle, inner cone radius, and two outer casing radius, while the exit diameter is imposed as a fixed constraint to represent engine-integration requirements. Computational fluid dynamics simulations are used to evaluate the compressible flow through the nozzle and to extract the main aerodynamic performance indicators. The optimization objectives are to maximize the discharge coefficient, maximize the gross thrust coefficient, maximize thrust, and minimize total pressure loss, expressed equivalently as improved exit total pressure recovery. A workflow combining parametric modeling, CFD simulation, sensitivity analysis, surrogate modeling, and multi-objective optimization is developed to identify improved nozzle geometries. The expected outcome is an optimized convergent nozzle configuration and a systematic methodology that can support future development of more complex exhaust systems, including convergent-divergent and variable-geometry nozzles.

2. Nozzle geometry and parametric design

The present study considers a convergent exhaust nozzle for gas turbine engine applications. The nozzle is modeled as an axisymmetric configuration, in which the meridional profile is defined in a two-dimensional plane and revolved about the engine centerline. This modeling approach is suitable for preliminary aerodynamic design because it reduces the geometric complexity while preserving the main flow characteristics of the convergent exhaust passage. The use of an axisymmetric representation is also consistent with common exhaust-nozzle design studies, where the internal contour and area distribution are the primary geometric factors controlling the flow acceleration and pressure-loss behavior.

The baseline nozzle geometry is developed from preliminary gas turbine exhaust design requirements. The exit diameter, D_e, is imposed as a fixed geometric constraint throughout the design and optimization process. This condition represents practical engine-integration requirements, where the nozzle exit size may be determined by the downstream installation envelope, engine casing, or required matching with adjacent engine components. Since the exit plane is also the minimum flow area in a convergent nozzle, the fixed exit diameter plays an important role in controlling the mass-flow capacity of the nozzle, particularly under choked-flow conditions [8]. Therefore, the optimization process focuses on modifying the internal contour and outer casing profile while maintaining the same prescribed exit diameter for all design candidates.

The nozzle flow passage is defined by the relative arrangement of the inner cone and the outer casing. The inner cone influences the flow development near the centerline region and affects the local acceleration, pressure distribution, and exit velocity profile. The outer casing defines the external boundary of the internal flow passage and controls the contraction of the nozzle area. Together, these surfaces determine the streamwise variation of the effective flow area, which directly affects the discharge coefficient, gross thrust coefficient, thrust, and total pressure loss. Previous nozzle and exhaust-system studies have shown that geometric features such as contour curvature, convergence angle, throat region, and area variation can significantly influence discharge behavior, pressure recovery, and thrust-related performance.

To enable systematic design exploration, the nozzle geometry is parameterized using five independent geometric variables: nozzle length, inner cone angle, inner cone radius, and two outer casing radius. These variables are selected because they directly influence the contraction rate of the flow passage, boundary-layer development, pressure distribution, and exit flow uniformity. Parametric geometry definition is widely used in aerodynamic design and optimization because it allows different design candidates to be generated systematically while maintaining geometric continuity and manufacturable shapes [4]. In the present work, the selected variables provide sufficient flexibility to modify the main nozzle contour while keeping the number of design variables suitable for CFD-based design exploration and surrogate-assisted optimization.

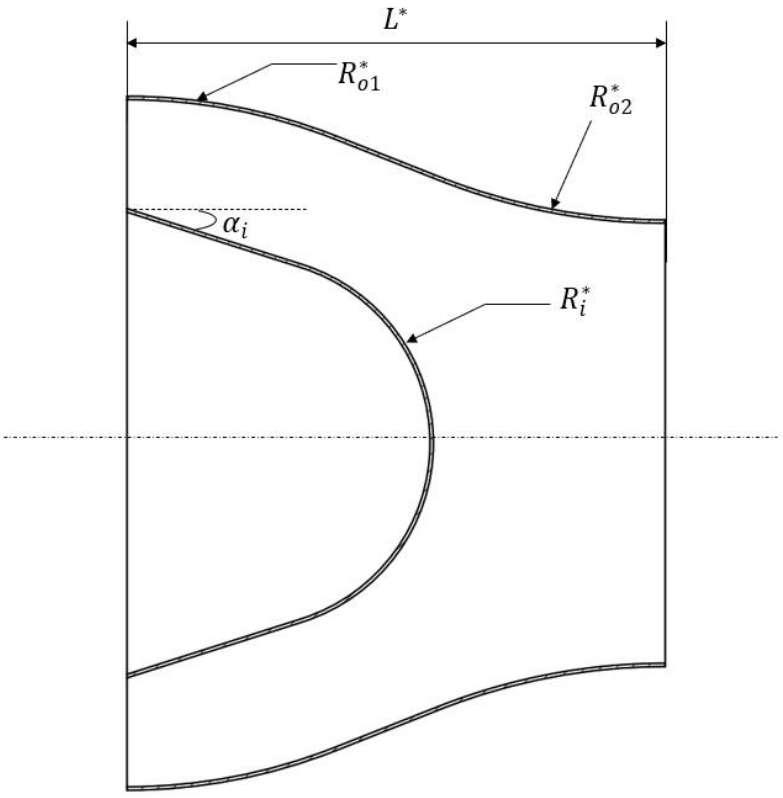


Figure 1 – Geometric variables of the convergent exhaust nozzle

For each design candidate, the nozzle contour is regenerated from the five input parameters while maintaining the fixed exit diameter. The parameter variations are limited by geometric feasibility and engine-integration requirements. Geometric constraints are applied to prevent invalid configurations, such as wall intersection, negative flow area, discontinuous curvature, excessive contraction, or unrealistic wall profiles. These constraints are necessary because invalid geometries can lead to poor mesh quality, numerical instability, or flow solutions that are not physically meaningful for gas turbine nozzle operation.

Table 1 – Geometric variables of the convergent nozzle

Symbol	Design variable	Description
L^*	Nozzle length	Axial length of the nozzle
α_i	Inner cone angle	Inclination angle of the cone
R_i^*	Inner cone radius	Radius at the tip of the inner cone
R_{o1}^*	Outer casing radius 1	Radius controlling upstream contour
R_{o2}^*	Outer casing radius 2	Radius controlling downstream outer contour

For the axisymmetric annular flow passage, the local effective flow area can be expressed as:

$$A(x)=\pi\left[R_0(x)^2-R_i(x)^2\right] \quad (1)$$

where $R_0(x)$ and $R_i(x)$ are the local outer and inner radius at the axial position x, respectively. The corresponding normalized area is defined as:

$$A^*(x)=\frac{A(x)}{A_e} \quad (2)$$

where A_e is the fixed exit area. The variation of A*(x) along the nozzle axis describes the contraction behavior of the nozzle and directly influences the acceleration of the exhaust gas. According to compressible-flow theory, the relationship between area variation and velocity change depends on the local Mach number; for subsonic flow, a reduction in area increases the flow velocity [1]. Therefore, the nozzle area distribution is a key geometric feature in convergent-nozzle design.

A smooth area variation is generally desirable because it can reduce strong pressure gradients, boundary-layer thickening, local separation tendency, and total pressure loss. However, overly mild contraction may increase the nozzle length and may not provide the desired compactness or acceleration performance. Conversely, excessive contraction or large cone angle may increase local losses and reduce discharge performance. Experimental and numerical studies on nozzle configurations have shown that convergence angle and throat-entry flow uniformity can affect discharge coefficient and thrust-related performance [9, 10]. Therefore, the selected geometric parameters must be optimized to obtain a balanced design rather than improving only one aerodynamic quantity.

The parametric geometry model provides the foundation for the subsequent CFD simulation and optimization process. By varying the five geometric parameters within their feasible ranges, a set of nozzle configurations is generated and evaluated under identical operating conditions. The resulting aerodynamic responses, including discharge coefficient, gross thrust coefficient, thrust, and total pressure loss, are then used for sensitivity analysis, surrogate modeling, and multi-objective optimization. This parametric approach allows the influence of each geometric variable to be quantified and supports the identification of an improved convergent nozzle geometry.

3. Computational domain and simulation

Computational fluid dynamics simulations were performed to evaluate the aerodynamic performance of the convergent nozzle configurations generated from the parametric geometry model. Since the nozzle geometry is axisymmetric, a two-dimensional axisymmetric numerical model was adopted. This approach represents the meridional section of the nozzle and reduces computational cost while retaining the main axial and radial flow characteristics of the exhaust passage. The computational-domain concept was developed with reference to axisymmetric nozzle–jet configurations reported in NASA validation resources, where a jet exits from a nozzle into an ambient region and the downstream flow development is included in the simulation domain [11, 12].

The computational domain consists of two main regions: the internal nozzle passage and the external ambient region downstream of the nozzle exit. The internal region includes the convergent flow

passage formed by the inner cone and the outer casing. The external region is included to allow the exhaust jet to develop after leaving the nozzle and to capture the interaction between the nozzle exit flow and the surrounding ambient pressure. The centerline of the model is defined as the axis of symmetry. The nozzle walls, inner cone surface, and outer casing surface are treated as solid boundaries. The downstream and outer boundaries of the ambient domain are positioned sufficiently far from the nozzle exit to reduce their influence on the near-field jet structure and nozzle performance evaluation.

The external ambient region has a rectangular shape, surrounding the nozzle, with the length of approximately 80 times the exit diameter and the width of 40 times the exit diameter. The nozzle inlet is extended by a 100 mm duct to ensure stability during the calculation process. Various CFD studies have shown that there is not much change in the calculation parameters and phenomena with and without this duct; however, the convergence of the computational model is significantly better. The boundary conditions here will be set according to the output conditions of the turbine. The domain's outlet is positioned far from the nozzle exit, at a distance 80 times the diameter of the nozzle exit. The boundary conditions here are set according to ambient conditions. To further increase the model's convergence capability, and to avoid backflow in the computational domain, the remaining outer surfaces surrounding the nozzle are set according to the conditions of a gentle airflow with a very low Mach number of 0.01. This flow is axial, with static pressure and total temperature equal to the ambient temperature.

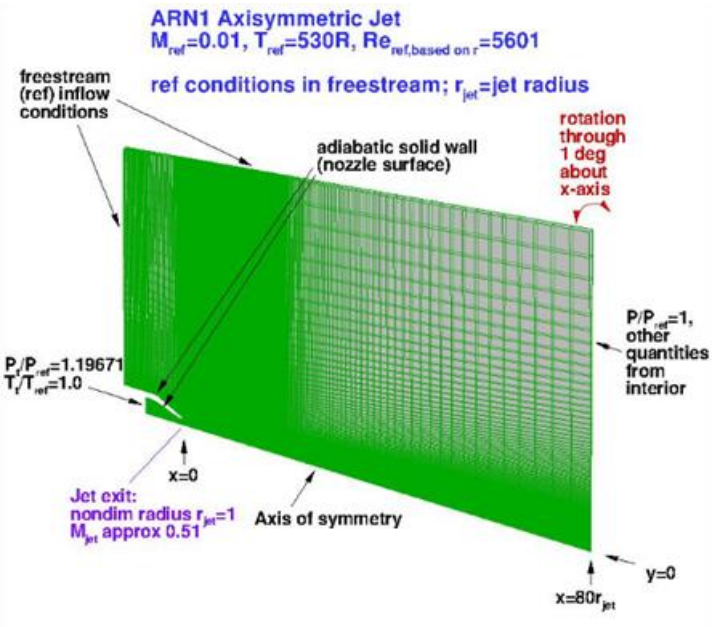


Figure 2 – NASA's axisymmetric jet model

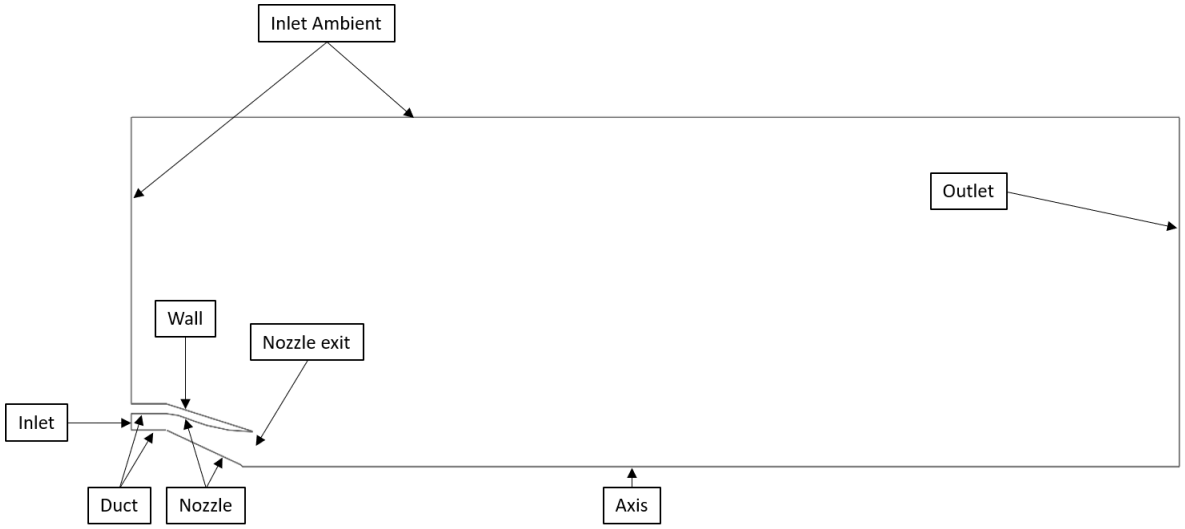


Figure 2 – 2D simulation domain

An unstructured quadrilateral mesh was generated for the two-dimensional axisymmetric domain. The mesh was refined near the nozzle wall, inner cone surface, exit region, and near-field jet region, where high velocity gradients and pressure variations are expected. Additional refinement was applied near the wall boundaries to improve the resolution of boundary-layer development and near-wall flow behavior. The same meshing strategy was applied consistently for all design candidates to ensure that the aerodynamic responses obtained from different geometries could be compared under equivalent numerical conditions. Mesh quality parameters, such as element skewness and orthogonality, were monitored during mesh generation to maintain numerical stability and solution accuracy.

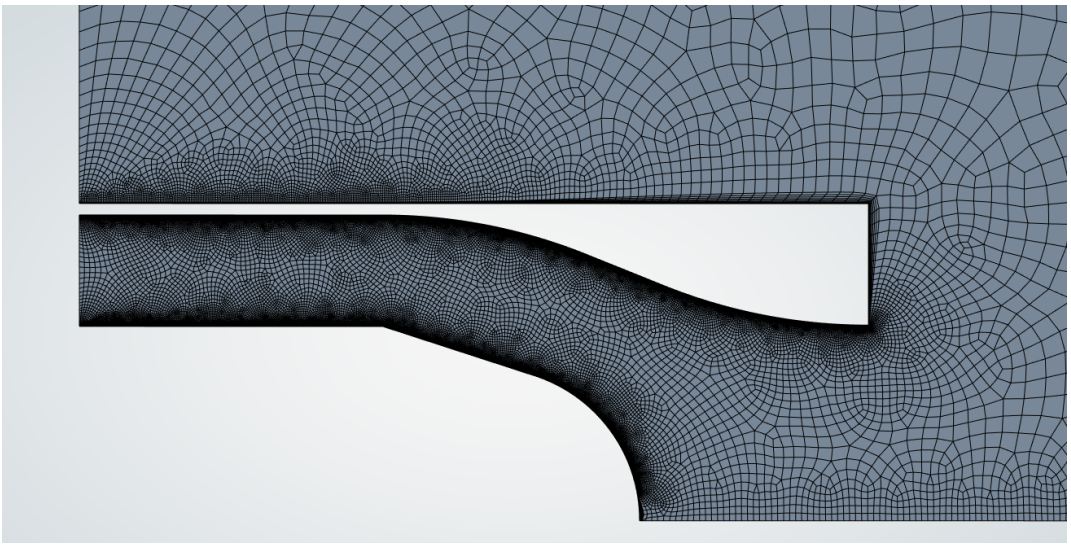


Figure 3 – Unstructured mesh of the nozzle and near-field jet region

After mesh generation, boundary conditions were assigned to represent the operating condition of the gas turbine exhaust nozzle. A pressure inlet boundary condition was applied at the nozzle inlet, where the inlet total pressure and total temperature were prescribed. This type of inlet condition is appropriate for compressible nozzle simulations because the upstream engine section is commonly represented by total flow properties. Pressure outlet boundary conditions were applied at the downstream and far-field boundaries of the ambient region to represent the surrounding environment and allow the exhaust jet to leave the computational domain. The nozzle walls, inner cone, and outer casing were modeled as stationary no-slip walls, while the centerline was specified as an axis boundary condition.

Table 2 – Boundary conditions

Region	Boundary type	Description
Inlet	Pressure inlet	Inlet total pressure and total temperature prescribed
Outlet	Pressure outlet	Ambient static pressure prescribed
Inlet ambient	Velocity inlet	Set to a very low Mach number of 0.01, with static pressure and total temperature equal to the ambient temperature.
Nozzle, wall, duct	Wall	Stationary no-slip wall condition
Axis	Axis	Axisymmetric boundary condition

The flow was modeled as steady, compressible, and turbulent. The Reynolds-averaged Navier–Stokes equations were solved with the k-ϵ turbulence model. This turbulence model was selected because it provides a practical balance between computational cost, robustness, and accuracy for engineering turbulent-flow simulations [13]. Since the present work involves multiple CFD evaluations for parametric analysis and optimization, computational efficiency is an important consideration. The use of a RANS-based turbulence model is therefore suitable for the current design-oriented study.

The numerical solution was initialized from the inlet condition and iterated until the residuals and monitored engineering quantities reached stable values. The monitored quantities included mass flow rate, thrust, discharge coefficient, gross thrust coefficient, and exit total pressure. These quantities were extracted from each CFD solution and used as output responses for sensitivity analysis, surrogate modeling, and multi-objective optimization.

Post-processing was conducted using both integral performance parameters and flow-field visualization. The integral parameters were used to compare the aerodynamic performance of different nozzle geometries, while contour plots of velocity, Mach number, static pressure, and total pressure were used to analyze the physical behavior of the flow. Particular attention was given to the exit velocity distribution, pressure recovery, total pressure loss, and possible unfavorable flow features such as excessive adverse pressure gradients or local separation tendency. This combination of quantitative performance evaluation and qualitative flow-field analysis provides the basis for selecting and validating the optimized nozzle geometry.

4. Performance Parameters and Theoretical Formulation

The aerodynamic performance of the convergent nozzle is evaluated using integral quantities extracted from the CFD solution and compared with ideal isentropic reference values. The main performance parameters considered in this study are mass flow rate, thrust, discharge coefficient, gross thrust coefficient, and total pressure loss. These quantities are selected because they directly represent the flow capacity, thrust generation, and aerodynamic loss characteristics of the nozzle.

For the actual CFD solution, the mass flow rate through the nozzle exit is obtained by integrating the normal mass flux over the exit plane:

$$\dot{m}_{CFD} = \int_{A_e} \rho V dA \tag{3}$$

where $\dot{m}_{CFD}$ is the actual mass flow rate, ρ is the local density, V is the velocity component normal to the exit plane, and A_{exit} is the nozzle exit area. For a two-dimensional axisymmetric simulation, this area integration is interpreted as the integration over the revolved exit surface.

The gross thrust of the nozzle is determined from the momentum flux and pressure force at the exit plane [14]. For a non-uniform exit flow, the actual gross thrust can be written as:

$$Fg, act = \int_{Ae} \rho(V \cdot n) V_x dA + \int_{Ae} (p - p_a) n_x dA \tag{4}$$

where F_g, act is the actual gross thrust, V_x is the axial velocity component, p is the local static pressure at the exit, p_a is the ambient pressure, and n_x is the axial component of the outward normal vector. For an axisymmetric nozzle with an exit plane normal to the axial direction, $V_n \approx V_x$ and $n_x = 1$, so the expression can be simplified as:

$$F_{g,act} = \int_{A_e} \rho\, V_x^2 dA + \int_{A_e} (p - p_a) dA \tag{5}$$

If the exit flow is assumed to be approximately uniform, the above relation reduces to the common one-dimensional thrust equation:

$$F_{g,act} = \dot{m}_{act}\, V_e + (p_e - p_a) A_e \tag{6}$$

where V_e and p_e are the area-averaged exit velocity and static pressure, respectively. For an ideally expanded nozzle, $p_e = p_a$, and the pressure thrust term becomes zero [2].

To evaluate nozzle performance independently of CFD numerical outputs, ideal isentropic reference quantities are required. The ideal mass flow rate is derived from the one-dimensional compressible-flow relation [16]. Starting from the definition of mass flow rate,

$$\dot{m} = \rho A V \tag{7}$$

and using the Mach number definition:

$$M = \frac{V}{a} \tag{8}$$

where a is the local speed of sound, the velocity can be written as:

$$V = M * a \tag{9}$$

For a perfect gas, the speed of sound is:

$$a = \sqrt{\gamma R T} \tag{10}$$

where γ is the specific heat ratio and R is the gas constant. Substituting this into the mass flow equation gives:

$$\dot{m} = \rho A\, M \sqrt{\gamma R T} \tag{11}$$

Using the ideal gas equation,

$$\rho = \frac{p}{RT} \tag{12}$$

the mass flow rate becomes:

$$\dot{m} = AMp \sqrt{\frac{\gamma}{RT}} \tag{13}$$

For isentropic flow, the static pressure and static temperature can be related to the total pressure and total temperature as:

$$\frac{T_t}{T} = 1 + \frac{\gamma - 1}{2} M^2 \tag{14}$$

and,

$$\frac{p_t}{p} = \left(1 + \frac{\gamma - 1}{2} M^2\right)^{\frac{\gamma}{\gamma - 1}} \tag{15}$$

where p_t and T_t are the total pressure and total temperature. Rearranging these equations gives:

$$T = \frac{T_t}{1 + \frac{\gamma - 1}{2} M^2} \tag{16}$$

$$p = \frac{p_t}{\left(1 + \frac{\gamma - 1}{2} M^2\right)^{\frac{\gamma}{\gamma - 1}}} \tag{17}$$

Substituting the isentropic pressure and temperature relations into the mass flow equation gives the ideal compressible mass flow rate:

$$\dot{m}_{ideal} = A \frac{p_t}{\sqrt{T_t}} \sqrt{\frac{\gamma}{R}} M \left(1 + \frac{\gamma - 1}{2} M^2\right)^{-\frac{\gamma + 1}{2(\gamma - 1)}} \tag{18}$$

This equation shows that the ideal mass flow rate depends on the flow area, total pressure, total temperature, gas properties, and Mach number [8, 15]. For a convergent nozzle operating under choked conditions, the Mach number at the minimum area reaches unity. Since the exit plane is the minimum area for a convergent nozzle, the ideal choked mass flow rate is obtained by setting $M = 1$ and $A = A_e$ [1]:

$$\dot{m}_{ideal,choked} = A_e \frac{p_{t,in}}{\sqrt{T_{t,in}}} \sqrt{\frac{\gamma}{R}} \left(\frac{2}{\gamma + 1}\right)^{\frac{\gamma + 1}{2(\gamma - 1)}} \tag{19}$$

where $p_{t,in}$ and $T_{t,in}$ are the inlet total pressure and total temperature. This value represents the maximum theoretical mass flow rate through the convergent nozzle under ideal isentropic conditions.

If the nozzle is not choked, the exit Mach number must first be determined from the isentropic pressure relation:

$$M_e = \sqrt{\frac{2}{\gamma - 1}\left[\left(\frac{p_{t,in}}{p_e}\right)^{\frac{\gamma - 1}{\gamma}} - 1\right]} \tag{20}$$

For an ideally expanded subsonic nozzle, p_e may be taken as the ambient pressure p_a. The corresponding ideal mass flow rate can then be calculated using the general compressible mass flow equation evaluated at $M = M_e$ and$A = A_e$.

The ideal exit temperature is obtained from the isentropic temperature relation:

$$T_{e,ideal} = \frac{T_{t,in}}{1 + \frac{\gamma - 1}{2} M_e^2} \tag{21}$$

and the ideal exit velocity is:

$$V_{e,ideal} = M_e \sqrt{\gamma R T_{e,ideal}} \tag{22}$$

Alternatively, the ideal exit velocity can be derived directly from the steady-flow energy equation. For adiabatic flow without shaft work, the total temperature is constant:

$$h_t = h + \frac{V^2}{2} \tag{23}$$

For a perfect gas,

$$h = c_p T \tag{24}$$

therefore,

$$c_p T_t = c_p T_e + \frac{V_e^2}{2} \tag{25}$$

Solving for the exit velocity gives:

$$V_{e,ideal} = \sqrt{2 c_p \left(T_{t,in} - T_{e,ideal}\right)} \tag{26}$$

The ideal gross thrust is then calculated as:

$$F_{g,ideal} = \dot{m} * V_{e,ideal} + \left(p_{e,ideal} - p_a\right) A_e = \dot{m}_i \sqrt{\frac{2\gamma}{\gamma - 1} RT \left[1 - \left(\frac{p_a}{p_{t,in}}\right)^{\frac{\gamma - 1}{\gamma}}\right]} \tag{27}$$

For a choked convergent nozzle, the ideal exit Mach number is $M_e = 1$. The corresponding ideal exit static temperature and pressure are:

$$T_{e,ideal} = T_{t,in} \left(\frac{2}{\gamma + 1}\right) \tag{28}$$

$$p_{e,ideal} = p_{t,in} \left(\frac{2}{\gamma + 1}\right)^{\frac{\gamma}{\gamma - 1}} \tag{29}$$

and the ideal exit velocity is:

$$V_{e,ideal} = \sqrt{\gamma R T_{e,ideal}} \tag{30}$$

These ideal quantities are used as reference values for evaluating the actual CFD performance.

The discharge coefficient is defined as the ratio between the actual mass flow rate obtained from CFD and the ideal isentropic mass flow rate:

$$c_d = \frac{\dot{m}_{act}}{\dot{m}_{ideal}} \tag{31}$$

A value of c_d close to unity indicates that the nozzle allows the required mass flow with relatively low blockage and aerodynamic loss. Values lower than unity indicate the effect of viscous losses, boundary-layer displacement thickness, flow non-uniformity, and other non-ideal effects.

The gross thrust coefficient is defined as the ratio between the actual gross thrust and the ideal gross thrust:

$$c_{fg} = \frac{F_{g,act}}{F_{g,ideal}} \tag{32}$$

A value of c_{fg} close to unity indicates that the nozzle converts the available pressure and thermal energy into thrust efficiently. A reduction in c_{fg} may be caused by total pressure loss, non-uniform exit velocity, pressure mismatch at the exit, separation, or viscous dissipation.

The total pressure loss is calculated by comparing the inlet total pressure with the mass-averaged exit total pressure:

$$\Delta p_t = p_{t,in} - \overline{p}_{t,e} \tag{33}$$

The corresponding total pressure loss coefficient or percentage loss is expressed as:

$$\Delta p_t^* = \frac{p_{t,in} - \overline{p}_{t,e}}{p_{t,in}} \tag{34}$$

or

$$\Delta p_t^*(\%) = \frac{p_{t,in} - \overline{p}_{t,e}}{p_{t,in}} \times 100 \tag{35}$$

where $\overline{p}_{t,e}$ is the mass-averaged total pressure at the nozzle exit. The mass-averaged exit total pressure is defined as:

$$\overline{p}_{t,e} = \frac{\int_{A_e} p_t \, \rho (V \cdot n) dA}{\int_{A_e} \rho \, (V \cdot n) dA} \tag{36}$$

This definition gives greater weight to the regions carrying higher mass flux and is therefore suitable for evaluating the effective pressure recovery of the nozzle exit flow.

In the present study, the optimization objectives are defined using these performance parameters. The discharge coefficient, gross thrust coefficient, and thrust are maximized, while total pressure loss is minimized. Equivalently, minimizing total pressure loss can be interpreted as maximizing exit total pressure recovery.

These objective functions provide a quantitative basis for comparing different nozzle geometries and identifying an optimized convergent nozzle configuration with improved flow capacity, thrust generation, and pressure recovery.

5. Design of Experiments, Sensitivity Analysis, and Multi-Objective Optimization

After the CFD methodology and performance parameters were defined, a surrogate-assisted multi-objective optimization workflow was developed to improve the aerodynamic performance of the convergent exhaust nozzle. The purpose of this workflow is to explore the relationship between the geometric design variables and the aerodynamic responses while reducing the number of full CFD simulations required. This approach is suitable for nozzle design because each CFD evaluation requires geometry generation, mesh generation, numerical solution, and post-processing.

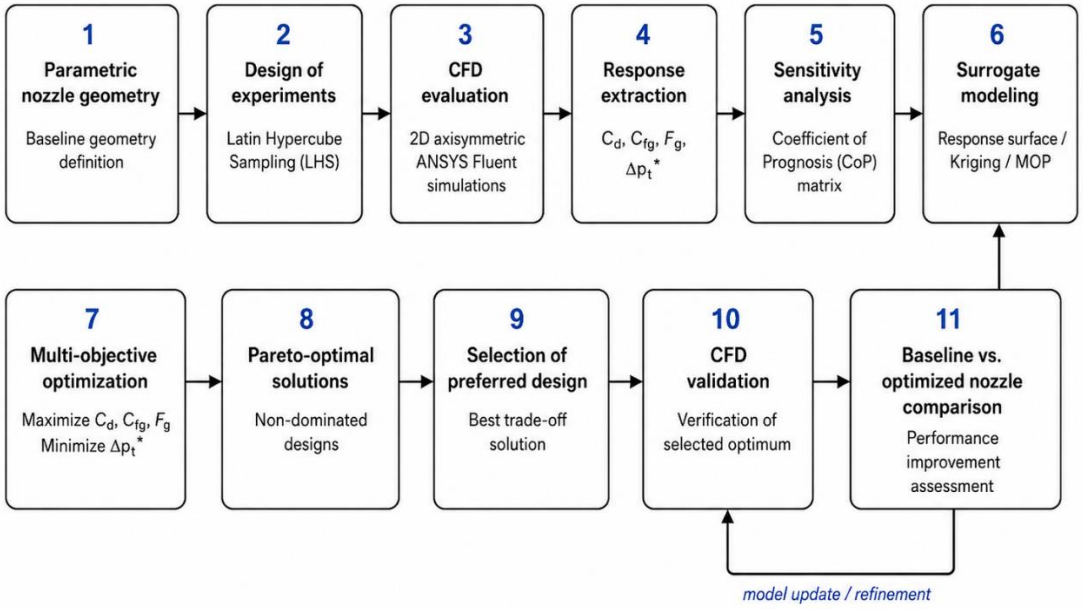


Figure 4 – Multi-objective optimization workflow

The design vector of the nozzle is defined as:

$$x = [L^*, \alpha_i, R_i^*, R_{o1}^*, R_{o2}^*]^T \tag{37}$$

where L^* is the nozzle length, α_i is the inner cone angle, R_i^* is the inner cone radius, and R_{o1}^* and R_{o2}^* are the outer casing radius. These five parameters form the input variables of the optimization process.

The aerodynamic response vector is defined as:

$$y = \left[C_d, C_{fg}, F_g, \Delta p_t^*\right]^T \tag{38}$$

where c_d is the discharge coefficient, c_{fg} is the gross thrust coefficient, F_g is the gross thrust, and Δp_t^* is the total pressure loss coefficient.

Table 3 – Input and output variables used in the optimization

Category	Parameter	Symbol	Objectives
Input	Nozzle length	L^*	Design variable
Input	Inner cone angle	α_i	Design variable
Input	Inner cone radius	R_i^*	Design variable
Input	Outer casing radius 1	R_{o1}^*	Design variable
Input	Outer casing radius 2	R_{o2}^*	Design variable
Output	Discharge coefficient	c_d	Maximize
Output	Gross thrust coefficient	c_{fg}	Maximize
Output	Gross thrust	F_g	Maximize
Output	Total pressure loss	Δp_t^*	Minimize

A design of experiments approach was first used to generate representative nozzle geometries within the feasible design space. Latin Hypercube Sampling was adopted because it provides an efficient distribution of sample points across the design-variable ranges and improves the coverage of the input space compared with simple random sampling [17]. Each sampled design point corresponds to one unique combination of the five geometric variables. The sampled geometries were then evaluated using the same CFD setup to ensure that the resulting aerodynamic responses could be compared under consistent numerical conditions.

The design matrix obtained from the sampling process can be written as

$$X = [x_1, x_2, \dots, x_N]^T \tag{39}$$

where N is the number of sampled design points. For each design point x_j, the CFD simulation provides the corresponding response vector y_j. The complete dataset obtained from the design of experiments is therefore expressed as:

$$D = \{(x_j, y_j), j = 1,2, \dots, N\} \tag{40}$$

This dataset provides the basis for sensitivity analysis, metamodel construction, and multi-objective optimization.

Sensitivity analysis was performed to identify the influence of each geometric parameter on the aerodynamic output responses. This step is important because not all design variables contribute equally to the performance of the nozzle. Parameters with strong influence on C_d, C_fg, thrust, or total pressure loss can be considered dominant design variables, while parameters with weaker influence have secondary effects. The sensitivity analysis therefore provides physical insight into how variations in nozzle length, inner cone angle, inner cone radius, and outer casing radii affect the flow capacity, thrust generation, and pressure recovery of the nozzle.

In this study, the sensitivity results are presented using the Coefficient of Prognosis matrix. The Coefficient of Prognosis, or CoP, is used to evaluate the predictive quality of a metamodel and the contribution of the input variables to the response prediction [18]. A higher CoP value indicates that the selected input variables and metamodel can predict the corresponding output response with better reliability. Therefore, the CoP matrix provides two useful pieces of information: the dominant geometric parameters affecting each aerodynamic response and the overall prediction quality of the surrogate model for each response.

The CoP value can be expressed conceptually as:

$$CoP = 1 - \frac{SS_E^{pred}}{SS_T} \tag{41}$$

where SS_E^{pred} is the prediction error estimated from cross-validation, and SS_T is the total variation of the response. A CoP value close to unity indicates good predictive capability, while a lower value indicates weaker prediction quality. In the present work, the CoP matrix is used to determine which design variables have the strongest influence on c_d, c_{fg}, F_g, and Δp_t^*, and to verify whether the response models are suitable for optimization.

Since direct CFD-based optimization is computationally expensive, surrogate models were constructed from the sampled CFD results. A surrogate model approximates the CFD response using a mathematical representation that is much faster to evaluate than the original CFD model. For each aerodynamic response, the surrogate approximation can be expressed as:

$$y_k \approx \hat{y}_{k(x)} \tag{42}$$

where y_k is the CFD-computed response, $\hat{y}_{k(x)}$ is the surrogate-predicted response, and k is the response index. Response surface and Kriging-based metamodels were considered because these methods are commonly used in engineering design optimization to approximate expensive numerical simulations [19, 20].

The accuracy of the surrogate model can be evaluated by comparing the predicted responses with the CFD-computed responses. One common indicator is the coefficient of determination, which can be written as

$$R^2 = 1 - \left(\frac{\sum_{j=1}^{N} \left(y_j - \hat{y}_j\right)^2}{\sum_{j=1}^{N} \left(y_j - \bar{y}\right)^2} \right) \tag{43}$$

where y_j is the CFD response at the j-th design point, $\hat{y}_j$ is the corresponding surrogate prediction, and $\bar{y}$ is the mean value of the CFD responses. A value of R^2 close to unity indicates that the surrogate model represents the CFD data with good accuracy. Together with the CoP matrix, this provides a basis for judging whether the metamodel is reliable enough for optimization.

The multi-objective optimization problem was formulated using the nozzle performance parameters as objective functions. The purpose of the optimization is to maximize the discharge coefficient, maximize the gross thrust coefficient, maximize gross thrust, and minimize normalized total pressure loss, and the geometric feasibility constraints imposed during the parametric geometry generation process. These constraints ensure that all candidate designs maintain a valid nozzle contour, fixed exit diameter, positive flow passage area, and physically realistic wall geometry.

For numerical implementation, the multi-objective problem can also be written in minimization form as:

$$minimize\, J(x) = \left[-c_{d(x)}, -c_{fg(x)}, -F_{g(x)}, \Delta p_t^*(x)\right] \tag{44}$$

where the negative signs are applied to c_d, c_{fg}, and F_g because these quantities are intended to be maximized.

The result of the multi-objective optimization is a set of Pareto-optimal solutions rather than a single universal optimum. A Pareto-optimal design is a design for which one objective cannot be improved without degrading at least one other objective. This is important for convergent nozzle optimization because the objectives may conflict with each other. For example, a geometry that increases thrust may also increase total pressure loss, while a smoother geometry that reduces loss may not produce the maximum thrust. Therefore, the final optimized design was selected from the Pareto-optimal set based on the best compromise between discharge capability, thrust generation, and pressure recovery.

After selecting the preferred optimized geometry, a final CFD simulation was performed using the same numerical setup as the baseline and sampled designs. The CFD-validated optimized result was then compared with the baseline nozzle to quantify the improvement in c_d, c_{fg}, thrust, and total pressure loss. This validation step ensures that the selected optimum is not only a surrogate-based prediction but also produces improved aerodynamic performance when evaluated using the full CFD model.

6. Results and Discussion

This section presents the aerodynamic results obtained from the baseline design, sensitivity analysis, surrogate model evaluation, multi-objective optimization, and CFD validation of the selected optimized nozzle. The performance of the nozzle is evaluated using the discharge coefficient, gross thrust coefficient, gross thrust, and normalized total pressure loss. The baseline design is used as the reference configuration, while the optimized design is assessed based on the improvement of the output responses and the flow-field characteristics of the final selected geometry.

6.1 Baseline Nozzle Performance

The baseline convergent nozzle was first evaluated using the CFD methodology described in the previous section. The purpose of this simulation was to establish a reference case for comparing the effect of parametric geometry variation and optimization. The main aerodynamic responses extracted from the baseline CFD result include the discharge coefficient, gross thrust coefficient, gross thrust, and normalized total pressure loss.

The baseline nozzle produced a discharge coefficient of 0.9837, indicating that the actual mass flow rate was close to the ideal isentropic mass flow rate. The gross thrust coefficient was 0.9758, showing the thrust-generation performance of the initial geometry relative to the ideal reference thrust. The normalized total pressure loss was 0.0106. These values provide the quantitative reference for evaluating the optimized nozzle configuration.

Table 4 – Baseline nozzle performance parameters

Parameter	Symbol	Baseline value
Discharge coefficient	c_d	0.9837
Gross thrust coefficient	c_{fg}	0.9758
Normalized total pressure loss	Δp_t^*	0.0106
Total pressure loss percentage	$\Delta p_t(\%)$	1.06 %

The baseline results show that the initial nozzle geometry already provides acceptable aerodynamic performance. However, the presence of total pressure loss and the difference between actual and ideal performance indicate that further improvement can still be achieved by modifying the nozzle contour. Therefore, the baseline response values are used as the basis for evaluating the effectiveness of the subsequent optimization process.

6.2 Sensitivity Analysis Using Coefficient of Prognosis Matrix

The sensitivity of the aerodynamic responses to the geometric design variables was evaluated using the Coefficient of Prognosis matrix. The input variables considered in the analysis were the nozzle length L^*, inner cone angle α_i, inner cone radius R_i^*, and outer casing radius R_{o1}^* and R_{o2}^*. The output responses were the discharge coefficient c_d, gross thrust coefficient c_{fg}, gross thrust F_g, and normalized total pressure loss Δp_t^*.

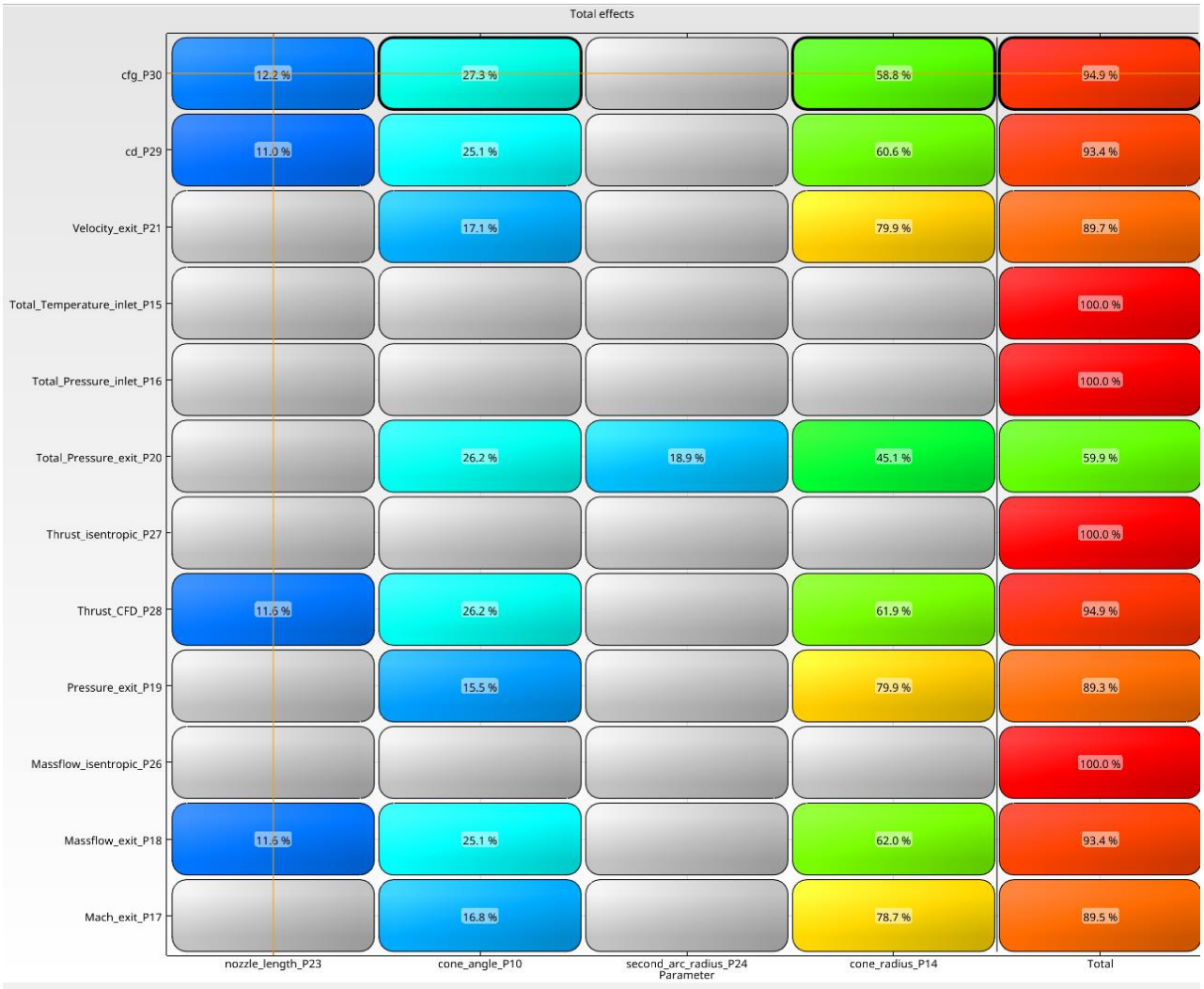


Figure 5 – Coefficient of Prognosis matrix for the geometric design variables and aerodynamic responses

The CoP matrix provides a compact representation of the relationship between the input variables and output responses. It identifies the dominant geometric parameters for each aerodynamic response and also indicates the prediction quality of the corresponding metamodel. A higher CoP value indicates that the response can be predicted with better reliability using the selected input variables and surrogate model.

From the CoP matrix, inner cone radius R_i^* and inner cone angle α_i were found to have the strongest influence on c_d and c_{fg}. This suggests that the mass-flow capacity and thrust coefficient are strongly affected by the main contraction behavior of the nozzle passage. In particular, parameters controlling the axial length and inner cone inclination can affect the acceleration process, wall pressure distribution, and exit velocity profile.

For the gross thrust response, the most influential parameters were inner cone radius R_i^*. This indicates that thrust is affected not only by the exit velocity but also by the combined influence of mass flow rate and pressure distribution inside the convergent passage. For the normalized total pressure loss, the dominant parameters were inner cone angle α_i, suggesting that pressure recovery is strongly related to the smoothness of the wall contour and the local area variation.

The sensitivity results show that the geometric parameters do not affect all performance responses in the same way. A parameter that improves the discharge coefficient or thrust coefficient may not necessarily minimize total pressure loss. This confirms that the nozzle design problem should be treated as a multi-objective optimization problem rather than a single-objective problem.

6.3 Surrogate Model Evaluation

Surrogate models were constructed from the CFD results obtained from the sampled design points. The purpose of the surrogate models was to approximate the relationship between the geometric input variables and aerodynamic output responses while reducing the computational cost of the optimization process. The predictive quality of the surrogate models was evaluated using the coefficient of determination and the full-model CoP values.

The coefficient of determination is expressed as

$$R^2 = 1 - \left(\frac{\sum(j=1)^N \left(y_j - \hat{y}_j\right)^2}{\sum(j=1)^N \left(y_j - \bar{y}\right)^2} \right) \tag{45}$$

where y_j is the CFD response at the j-th design point, $\hat{y}_j$ is the surrogate-predicted response, ȳ is the mean value of the CFD responses, and N is the total number of design points.

The surrogate model accuracy for each aerodynamic response is summarized in Table 5. The results show that the metamodels provide [good / acceptable] prediction accuracy for the main nozzle performance responses. The responses [insert response names] showed the highest prediction accuracy, while [insert response name] showed relatively lower accuracy due to [possible nonlinear behavior / local flow sensitivity / stronger interaction between variables].

Table 5 – Surrogate model accuracy for aerodynamic responses

Response	Surrogate model type	Full-model CoP	Prediction quality
c_d	MOP-selected metamodel	0.95	High
c_{fg}	MOP-selected metamodel	0.93	High
F_g	MOP-selected metamodel	0.91	High
Δp_t^*	MOP-selected metamodel	0.84	Good

6.4 Multi-Objective Optimization Results

The multi-objective optimization was performed with four objectives: maximizing discharge coefficient, maximizing gross thrust coefficient, maximizing gross thrust, and minimizing normalized total pressure loss.

The percentage improvement of a performance parameter is calculated as

$$Improvement(\%) = \left(\frac{Q_{opt} - Q_{base}}{Q_{base}} \right) \times 100 \tag{46}$$

where Q_{base} is the baseline value and Q_{opt} is the optimized value.

For total pressure loss, the reduction percentage is calculated as

$$Reduction(\%) = \left(\frac{\Delta p_{t,base}^* - \Delta p_{t,opt}^*}{\Delta p_{t,base}^*} \right) \times 100 \tag{47}$$

where $\Delta p_{t,base}^*$ and $\Delta p_{t,opt}^*$ are the normalized total pressure losses of the baseline and optimized nozzles, respectively.

Table 6 – Comparison between baseline and optimized nozzle performance

Parameter	Baseline	Optimized	Change
c_d	0.9837	0.9986	1.5%
c_{fg}	0.9758	0.9868	1.1%
F_g	1	1.0209	2.09%
Δp_t^*	0.0106	0.0091	14%
Δp_t (%)	1.06 %	0.91%	14%

The comparison confirms that the optimized geometry improves the aerodynamic performance of the convergent nozzle while maintaining the fixed exit diameter constraint. The improvement is achieved through modification of the internal contour and casing geometry rather than changing the exit size.

6.5 CFD Validation of the Optimized Design

To verify the optimization result, the selected optimized nozzle geometry was re-evaluated using CFD. The CFD validation result was compared with the surrogate prediction to assess whether the selected optimum remains valid when evaluated using the full numerical model.

The prediction error is calculated as

$$Error(\%) = \frac{|Q_{CFD} - Q_{pred}|}{Q_{CFD}} \times 100 \tag{48}$$

where Q_{CFD} is the CFD-validated value and Q_{pred} is the surrogate-predicted value.

Table 7 – CFD validation of the selected optimized nozzle

Response	Surrogate prediction	CFD validation	Error (%)
c_d	0.9986	0.992	0.6%
c_{fg}	0.9868	0.9817	0.5%
F_g	1.0209	1.0126	0.8%
Δp_t^*	0.0091	0.0093	2.1%

The prediction errors for the selected optimized design were within 5%, indicating that the surrogate model provided acceptable prediction accuracy. Therefore, the selected nozzle geometry can be considered a reliable optimized configuration within the investigated design space.

6.6 Flow-Field Analysis of the Optimized Nozzle

The flow-field characteristics of the selected optimized nozzle were analyzed to provide physical interpretation of the optimized performance. Since the quantitative comparison between the baseline and optimized configurations is already presented in Table 6, the flow-field visualization in this subsection focuses on the final optimized geometry.

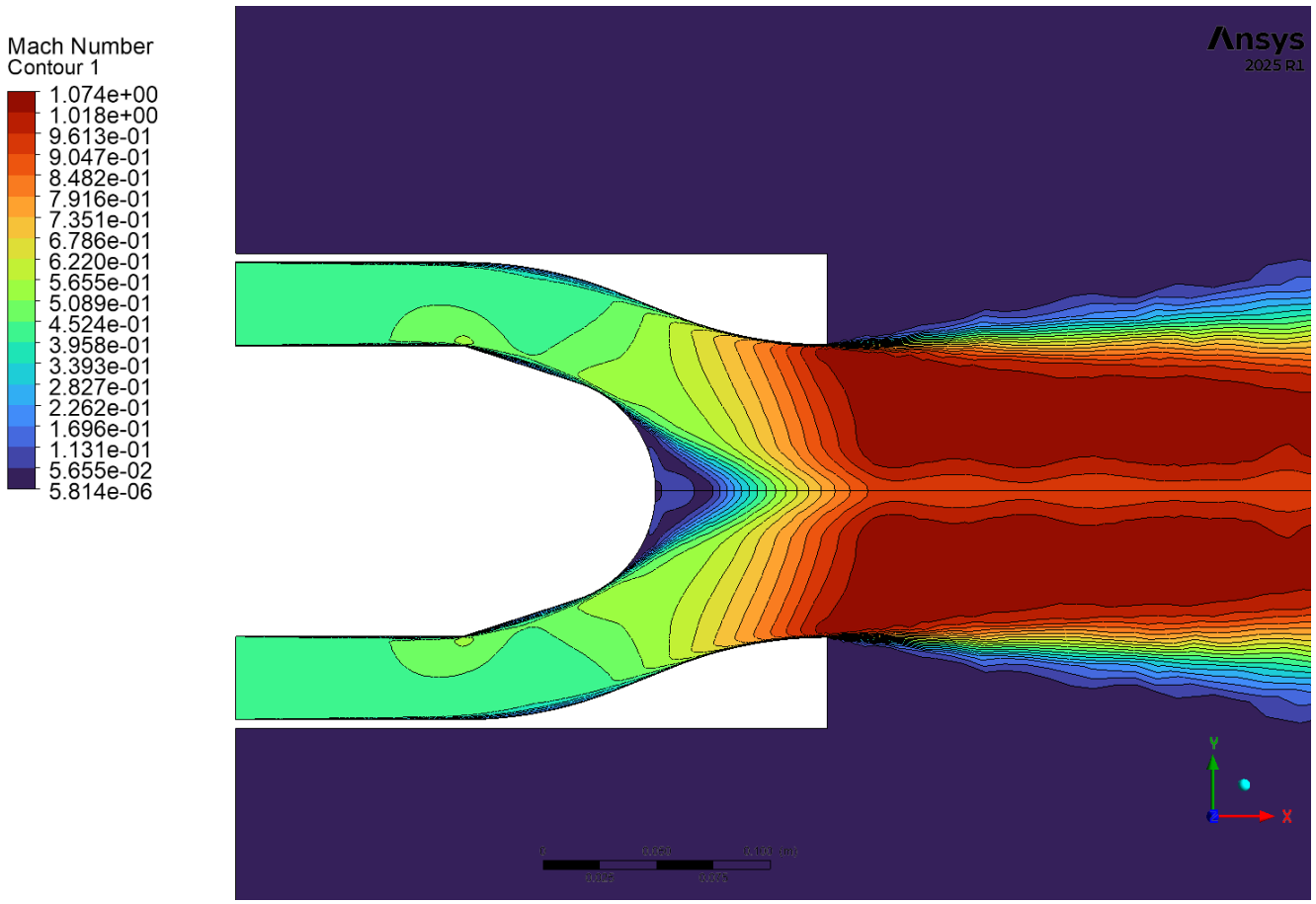


Figure 6 – Mach number contour of the optimized nozzle.

The Mach number contour shows that the optimized nozzle produces smooth acceleration of the exhaust flow toward the exit. The flow remains well guided along the convergent passage, and no significant unfavorable flow behavior is observed under the investigated operating condition. A smooth acceleration process is desirable because it supports high discharge performance and contributes to improved thrust generation.

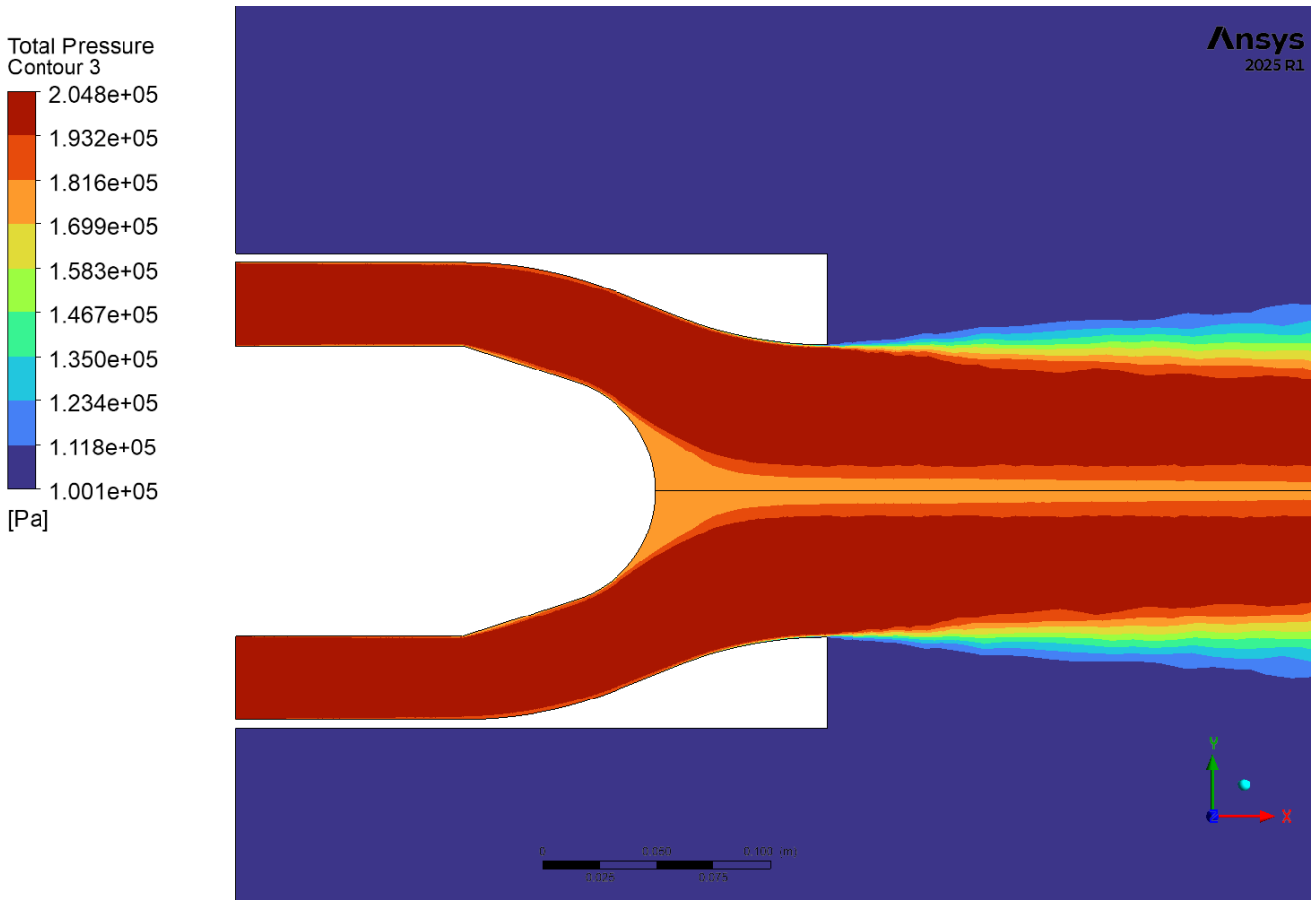


Figure 7 – Total pressure contour of the optimized nozzle.

The total pressure contour of the optimized nozzle shows the distribution of pressure loss along the flow passage. The optimized geometry maintains good pressure recovery, with the main total pressure reduction occurring gradually along the nozzle rather than being concentrated in a localized region. This behavior indicates that the optimized wall contour helps reduce excessive pressure gradients and limits unnecessary aerodynamic loss.

Overall, the optimized nozzle achieves improved aerodynamic performance through a better balance between flow acceleration and pressure recovery. The quantitative comparison shows improvements in c_d, c_{fg}, and F_g, together with a reduction in Δp_t^*. The optimized flow-field results further support the conclusion that the selected geometry provides smooth internal flow behavior and acceptable pressure-loss characteristics.

7. Conclusion

This study presented a parametric design and surrogate-assisted multi-objective optimization approach for a convergent exhaust nozzle used in gas turbine engine applications. The nozzle geometry was defined using five main design variables, including the normalized nozzle length, inner cone angle, normalized inner cone radius, and two normalized outer casing radii, while the exit diameter was maintained as a fixed geometric constraint. This allowed the nozzle contour to be modified systematically while preserving the required engine-integration condition.

A two-dimensional axisymmetric CFD model was developed to evaluate the aerodynamic performance of each nozzle configuration. The main performance parameters considered in this study were the discharge coefficient, gross thrust coefficient, gross thrust, and normalized total pressure loss. These quantities were selected because they represent the flow capacity, thrust-generation capability, and pressure-recovery behavior of the nozzle.

The design of experiments and surrogate modeling process provided an efficient method for exploring the design space without requiring exhaustive CFD simulations. The Coefficient of Prognosis matrix was used to evaluate the influence of the geometric variables on the aerodynamic responses and to assess the prediction quality of the metamodels. The results showed that the nozzle performance is strongly affected by the geometric parameters controlling the contraction behavior, inner cone shape, and casing curvature.

The multi-objective optimization produced a set of Pareto-optimal nozzle configurations. From these solutions, a preferred optimized design was selected based on the best compromise between high discharge coefficient, high gross thrust coefficient, high gross thrust, and low total pressure loss. The optimized geometry was then re-evaluated using CFD to verify the surrogate-based prediction. The comparison between the baseline and optimized designs showed that the proposed workflow can improve the aerodynamic performance of the convergent nozzle.

Overall, the results demonstrate that parametric geometry definition combined with CFD simulation, sensitivity analysis, surrogate modeling, and multi-objective optimization is an effective methodology for convergent exhaust nozzle design. The proposed approach provides useful design insight into the relationship between nozzle geometry and aerodynamic performance and can support the development of improved exhaust systems for gas turbine engines.

8. Copyright Statement

The authors confirm that they, and/or their company or organization, hold copyright on all of the original material included in this paper. The authors also confirm that they have obtained permission, from the copyright holder of any third party material included in this paper, to publish it as part of their paper. The authors confirm that they give permission, or have obtained permission from the copyright holder of this paper, for the publication and distribution of this paper as part of the ICAS proceedings or as individual off-prints from the proceedings

References

[1] National Aeronautics and Space Administration. *Mass flow choking*. NASA Glenn Research Center, *Beginner's Guide to Aeronautics*, online resource, accessed 13 June 2026.

[2] National Aeronautics and Space Administration. *Thrust equations summary*. NASA Glenn Research Center, *Beginner's Guide to Aeronautics*, online resource, accessed 13 June 2026.

[3] Matesanz-García J, Piovesan T and MacManus DG. *Aerodynamic optimization of the exhaust system of an aft-mounted boundary layer ingestion propulsor. International Journal of Numerical Methods for Heat and Fluid Flow*, Vol. 33, No. 4, pp 1295-1318, 2023.

[4] Goulos I, Otter J, Stankowski T, MacManus D, Grech N and Sheaf C. *Design optimisation of separate-jet exhausts for the next generation of civil aero-engines*. *The Aeronautical Journal*, Vol. 122, No. 1256, pp 1586-1605, 2018.

[5] Bagy S, Lallia M, Coat P, Mohammadi B and Méheut M. *Aerodynamic shape optimization of aircraft engine nozzles based on Computer-Aided Design.* Proc AIAA Scitech 2020 Forum, Orlando, Florida, USA, AIAA Paper 2020-2247, pp 1-14, 2020.

[6] Zhang S, Yang Q, Wang R and Wang X. *Multi-Objective Bayesian Optimization Design of Elliptical Double Serpentine Nozzle*. Aerospace, Vol. 11, No. 1, Article 48, 2024.

[7] Yerlikaya B. *Adjoint based optimization of supersonic converging diverging nozzle*. MSc thesis, Middle East Technical University, 2019.

[8] National Aeronautics and Space Administration. *Mass flow rate equations*. NASA Glenn Research Center, Beginner's Guide to Aeronautics, online resource, accessed 13 June 2026.

[9] Carson GT and Lee EE. *Experimental and Analytical Investigation of Axisymmetric Supersonic Cruise Nozzle Geometry at Mach Numbers from 0.60 to 1.30*. NASA Technical Paper, NASA Langley Research Center, 1981.

[10] Hamedi-Estakhrsar MH, Mahdavy-Moghaddam H and Jahromi M. *Investigation of effects of convergence and divergence half-angles on the performance of a nozzle for different operating conditions*. Journal of the Brazilian Society of Mechanical Sciences and Engineering, Vol. 40, No. 7, Article 353, 2018.

[11] National Aeronautics and Space Administration. *ASJ: Axisymmetric Subsonic Jet*. NASA Turbulence Modeling Resource, online resource, accessed 13 June 2026.

[12] National Aeronautics and Space Administration. *Supersonic Axisymmetric Jet Flow: Study #1*. NPARC Alliance Validation Archive, NASA Glenn Research Center, online resource, accessed 13 June 2026.

[13] National Aeronautics and Space Administration. *Turbulence Modeling Resource*. NASA Langley Research Center, online resource, accessed 13 June 2026.

[14] National Aeronautics and Space Administration. *Thrust equation*. NASA Glenn Research Center, Beginner's Guide to Aeronautics, online resource, accessed 13 June 2026.

[15] National Aeronautics and Space Administration. *Isentropic flow equations*. NASA Glenn Research Center, Beginner's Guide to Aeronautics, online resource, accessed 13 June 2026.

[16] National Aeronautics and Space Administration. *Converging/Diverging nozzle*. NASA Glenn Research Center, Beginner's Guide to Aeronautics, online resource, accessed 13 June 2026.

[17] McKay MD, Beckman RJ and Conover WJ. *A comparison of three methods for selecting values of input variables in the analysis of output from a computer code*. Technometrics, Vol. 21, No. 2, pp 239-245, 1979.

[18] Most T and Will J. *Sensitivity analysis using the Metamodel of Optimal Prognosis*. arXiv preprint, arXiv:2408.03590, 2024.

[19] Han ZH and Zhang KS. *Surrogate-Based Optimization*. In: Roeva O, editor. Real-World Applications of Genetic Algorithms, InTech, pp 343-362, 2012.

[20] Mukhtar A, Pitroda A, Patel V and Shah S. *A machine learning-based comparative analysis of surrogate models for design optimization*. Heliyon, Vol. 9, No. 7, Article e18197, 2023.